

# J|A|C|S

## A R T I C L E S

Published on Web 00/00/0000

### Molecular Engineering and Measurements To Test Hypothesized Mechanisms in Single Molecule Conductance Switching

Amanda M. Moore,<sup>†</sup> Arrelaine A. Dameron,<sup>†</sup> Brent A. Mantooth,<sup>†</sup> Rachel K. Smith,<sup>†</sup>  
Daniel J. Fuchs,<sup>†</sup> Jacob W. Ciszek,<sup>‡</sup> Francisco Maya,<sup>‡</sup> Yuxing Yao,<sup>‡</sup>  
James M. Tour,<sup>\*,‡</sup> and Paul S. Weiss<sup>\*,†</sup>

*Contribution from the Departments of Chemistry and Physics, The Pennsylvania State  
University, University Park, Pennsylvania 16802-6300, and Department of Chemistry and  
Center for Nanoscale Science and Technology, Rice University, Houston, Texas 77005*

Received August 22, 2005; E-mail: tour@rice.edu; stm@psu.edu

**Abstract:** Six customized phenylene-ethynylene-based oligomers have been studied for their electronic properties using scanning tunneling microscopy to test hypothesized mechanisms of stochastic conductance switching. Previously suggested mechanisms include functional group reduction, functional group rotation, backbone ring rotation, neighboring molecule interactions, bond fluctuations, and hybridization changes. Here, we test these hypotheses experimentally by varying the molecular designs of the switches; the ability of the molecules to switch via each hypothetical mechanism is selectively engineered into or out of each molecule. We conclude that hybridization changes at the molecule–surface interface are responsible for the switching we observe.

#### Introduction

With the physical limitations of semiconductor microelectronic fabrication in sight, new approaches are needed to obtain ever smaller and faster devices. The ultimate limitation lies in single molecule electron transport through controllable, connectable systems. Feasibility of these molecular devices will lie in our ability to understand specific properties of molecules acting individually or in bundles and to exploit these properties in the creation of a new class of devices.<sup>1</sup> Molecules containing a high degree of  $\pi$ -conjugation have been of great interest for their potential use in fabricating molecular electronic devices due to their electron delocalization leading to low barriers for electron transport.<sup>2–4</sup> Conjugated molecules studied have included polythiophenes, polyphenylenes, polyanalines, polyphenylenevinyls, and oligo(phenylene-ethynylene)s (OPEs), which have shown interesting properties including conductance switching.<sup>5–12</sup>

One of the most useful aspects of using molecules for device fabrication is the ability to synthesize and to modify them to have controllable and reproducible properties (i.e., each molecule is precisely the same).<sup>2,13</sup> Highly conjugated molecules have been studied by a variety of techniques analyzing ensembles of many molecules down even to single molecules. Using nanopore junctions, bundles of functionalized OPE molecules have been shown to exhibit hysteretic conductance switching.<sup>14–16</sup> In break junctions<sup>17–20</sup> and crossed-wire tunneling junctions,<sup>21</sup> few to single molecules have been analyzed for their conductance and contact dependence. Finally, at the single molecule level, we and others have used scanning tunneling microscopy (STM) to study conductance switching for OPE molecules.<sup>5–8</sup>

<sup>†</sup> The Pennsylvania State University.

<sup>‡</sup> Rice University.

- (1) Mantooth, B. A.; Weiss, P. S. *Proc. IEEE* **2003**, *91*, 1785.
- (2) Fischer, C. M.; Burghard, M.; Roth, S. *Mater. Sci. Forum* **1995**, *191*, 149.
- (3) Magoga, M.; Joachim, C. *Phys. Rev. B* **1997**, *56*, 4722.
- (4) Seminario, J. M.; Derosa, P. A. *J. Am. Chem. Soc.* **2001**, *123*, 12418.
- (5) Donhauser, Z. J.; Mantooth, B. A.; Kelly, K. F.; Bumm, L. A.; Monnell, J. D.; Stapleton, J. J.; Price, D. W.; Rawlett, A. M.; Allara, D. L.; Tour, J. M.; Weiss, P. S. *Science* **2001**, *292*, 2303.
- (6) Donhauser, Z. J.; Mantooth, B. A.; Pearl, T. P.; Kelly, K. F.; Nanayakkara, S. U.; Weiss, P. S. *Jpn. J. Appl. Phys.* **2002**, *41*, 4871.
- (7) Lewis, P. A.; Inman, C. E.; Yao, Y. X.; Tour, J. M.; Hutchison, J. E.; Weiss, P. S. *J. Am. Chem. Soc.* **2004**, *126*, 12214.
- (8) Lewis, P. A.; Inman, C. E.; Yao, Y. X.; Tour, J. M.; Hutchison, J. E.; Weiss, P. S. *J. Am. Chem. Soc.*, in press.
- (9) Dameron, A. A.; Ciszek, J. W.; Tour, J. M.; Weiss, P. S. *J. Phys. Chem. B* **2004**, *108*, 16761.

- (10) Wassel, R. A.; Fuierer, R. R.; Kim, N.; Gorman, C. B. *Nano Lett.* **2003**, *3*, 1617.
- (11) Ramachandran, G. K.; Hopson, T. J.; Rawlett, A. M.; Nagahara, L. A.; Primak, A.; Lindsay, S. M. *Science* **2003**, *300*, 1413.
- (12) Sakaguchi, H.; Matsumura, J.; Gong, H. *Nat. Mater.* **2004**, *3*, 551.
- (13) Tour, J. M.; Rawlett, A. M.; Kozaki, M.; Yao, Y. X.; Jagessar, R. C.; Dirk, S. M.; Price, D. W.; Reed, M. A.; Zhou, C. W.; Chen, J.; Wang, W. Y.; Campbell, I. *Chem.-Eur. J.* **2001**, *7*, 5118.
- (14) Reed, M. A.; Chen, J.; Rawlett, A. M.; Price, D. W.; Tour, J. M. *Appl. Phys. Lett.* **2001**, *78*, 3735.
- (15) Mathews, R. H.; Sage, J. P.; Gerhard Sollner, T. C. L.; Calawa, S. D.; Chen, C.-L.; Mahoney, L. J.; Maki, P. A.; Molvar, K. M. *Proc. IEEE* **1999**, *87*, 596.
- (16) Zhou, C.; Deshpande, M. R.; Reed, M. A.; Jones, L.; II; Tour, J. M. *Appl. Phys. Lett.* **1997**, *71*, 611.
- (17) Muller, C. J.; Krans, J. M.; Todorov, T. N.; Reed, M. A. *Phys. Rev. B* **1996**, *53*, 1022.
- (18) Muller, C. J.; Vleeming, B. J.; Reed, M. A.; Lamba, J. J. S.; Hara, R.; Jones, L.; II; Tour, J. M. *Nanotechnology* **1996**, *7*, 409.
- (19) Reed, M. A.; Zhou, C.; Muller, C. J.; Burgin, T. P.; Tour, J. M. *Science* **1997**, *278*, 252.
- (20) Reichert, J.; Weber, H. B.; Mayor, M.; von Lohneysen, H. *Appl. Phys. Lett.* **2003**, *82*, 4137.
- (21) Kushmerick, J. G.; Holt, D. B.; Yang, J. C.; Naciri, J.; Moore, M. H.; Shashidhar, R. *Phys. Rev. Lett.* **2002**, *89*, 086802.

Stochastic conductance switching is an interesting, useful, and reproducible property observed by STM for single OPE and other molecules inserted into a host *n*-alkanethiolate self-assembled monolayer (SAM).<sup>5,6,22</sup> A molecule observed in a high conductance or “on” state appears to protrude several angstroms from the SAM in STM images, while a molecule in the low conductance or “off” state protrudes only slightly or not at all. The inserted molecules stochastically switch or in some cases can be driven between conductance states and are stable within each state for time periods of milliseconds to many hours depending on the packing of the host matrix around the inserted molecule and the nature of the surrounding matrix. These lifetimes are measured by acquiring several successive images over the same area and extracting the apparent height for individual molecules or by recording the time history profile over a single inserted molecule.<sup>23</sup> The time spent in each conductance state has been shown to be strongly dependent on the rigidity of, and interactions with, the surrounding matrix.<sup>5–8</sup> In addition, a limited ability to control the conductance switching of these molecules has been demonstrated using an applied electric field<sup>5,7,8</sup> as well as bias-dependent, matrix-mediated switching through the use of amide-containing alkanethiols in which dipole and hydrogen-bonding interactions play a role and are not found in *n*-alkanethiolate matrixes.<sup>7,8</sup>

We note that conductance switching imaged by STM is a process different than negative differential resistance (NDR) observed in nanopores and some other testbeds, but remains a subject of controversy.<sup>13,24–29</sup> Nevertheless, similar hypotheses have been suggested to describe both conductance switching and NDR, because these phenomena have only recently been attributed to separate mechanisms.<sup>30</sup> Both theoretical and experimental works have attempted to explain conductance changes through a variety of schemes, including reduction of functional groups,<sup>31</sup> rotation of functional groups,<sup>32</sup> backbone phenyl ring rotations,<sup>33</sup> neighboring molecule interactions,<sup>34,35</sup> bond fluctuations,<sup>11</sup> and changes in bond hybridization.<sup>5,6,36,37</sup> In the reduction scheme, Seminario et al. suggested that applying a reducing potential to nitro- and amino-functionalized molecules can reduce the molecule, thereby increasing conduction.<sup>31</sup>

Di Ventra et al. suggested that the rotational plane of the ligands (i.e., nitro-group on functionalized OPEs), not reduction, affects molecular conductance.<sup>32</sup> Conversely, Brédas and co-workers analyzed the rotation of the middle OPE phenyl ring, concluding that constricting the rotation of the ring inhibits changes in conductance.<sup>33</sup> Further theoretical work has discussed the possibility that motion and interactions with nearby molecules in close proximity affect the conductance of the switches.<sup>34,35</sup> For bond fluctuations, Ramachandran et al. suggested that conductance switching is caused by bond-breaking at the S–Au interface where the molecule is in the “off” state (the molecule or nanoparticle is not imaged by STM) when it is not covalently attached to the Au substrate.<sup>11</sup> We have previously suggested that a change in hybridization between the conjugated molecules and the substrate results in our observed stochastic changes in conductance.<sup>5,6</sup> The hybridization change can occur through surface reconstruction or a change in the alignment of the molecule with the surface. Sellers et al. suggest that S–Au interactions can bind at 180° (perpendicular to the surface) having sp hybridization, while those that are at 104° (tilted) have sp<sup>3</sup> hybridization; sp<sup>3</sup> hybridization is favored for alkanethiols.<sup>36</sup> The barrier for this change in tilt of the molecule has been calculated to be 0.11 eV for alkanethiols.<sup>36,37</sup> Bauschlicher et al. have calculated conductance changes for benzene-1,4-dithiol molecules dependent on the conformation of the molecules with respect to the gold electrodes to which they are attached, as well as their bonding coordination.<sup>38</sup>

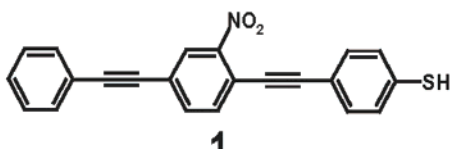


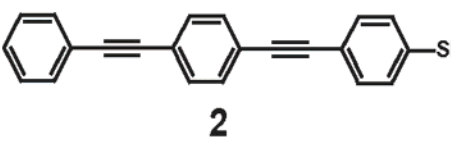
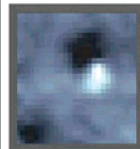

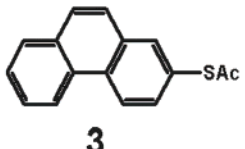


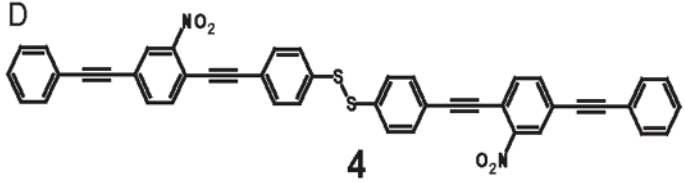
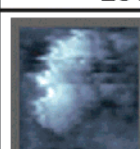
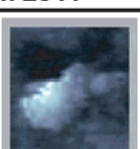
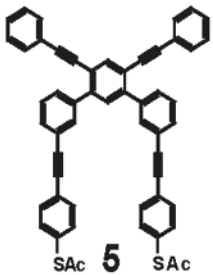


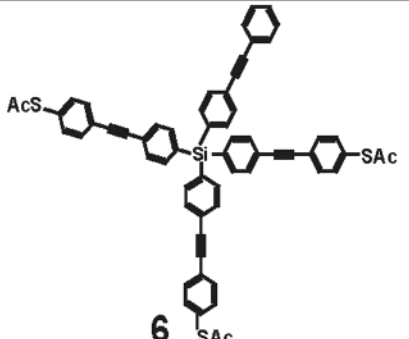


Here, we show STM data for conductance switching for a variety of conjugated molecules, shown in Figure 1. By specifically engineering the molecular design, we experimentally test each of the proposed switching mechanisms.

## Experimental Section

**Sample Preparation.** Host matrixes of *n*-alkanethiolate SAMs were prepared on commercially obtained Au{111} on mica (Molecular Imaging, Phoenix, AZ). The Au{111} substrates were annealed using a hydrogen flame followed immediately by SAM deposition. The host SAM was prepared by immersing the substrate in a 1 mM solution of *n*-alkanethiol in ethanol for 24 h. The lengths of the alkanethiolate chains presented here vary between 8 and 12 carbons, using only even numbers of carbons due to the more favorable van der Waals interactions and the orientation of the chain terminal group.<sup>45</sup> Following the insertion procedure (described below), vapor annealing was sometimes performed to tighten the host matrix, and to favor insertion of only single conjugated molecules. This was done with a neat *n*-alkanethiol (the same chain length as was used to create the original SAM) vapor anneal at 80 °C for 2 h in a sealed vial. Vapor annealing was used to add molecules to the matrix from the gas phase, while minimizing the exchange processes that occur during solution-phase annealing.<sup>5,6,46</sup> Following SAM deposition, the substrates were rinsed with ethanol and dried under a stream of nitrogen.

- (22) Cygan, M. T.; Dunbar, T. D.; Arnold, J. J.; Bumm, L. A.; Shedlock, N. F.; Burgin, T. P.; Jones, L. II; Allara, D. L.; Tour, J. M.; Weiss, P. S. *J. Am. Chem. Soc.* **1998**, *120*, 2721.
- (23) Donhauser, Z. J., Probing Nanoscale Electronics Using Scanning Tunneling Microscopy. Ph.D. Thesis, The Pennsylvania State University, 2003.
- (24) Chen, J.; Reed, M. A.; Rawlett, A. M.; Tour, J. M. *Science* **1999**, *286*, 1550.
- (25) Chen, J.; Wang, W.; Reed, M. A.; Rawlett, A. M.; Price, D. W.; Tour, J. M. *Appl. Phys. Lett.* **2000**, *77*, 1224.
- (26) Amlani, I.; Rawlett, A. M.; Nagahara, L. A.; Tsui, R. K. *Appl. Phys. Lett.* **2002**, *80*, 2761.
- (27) Rawlett, A. M.; Hopson, T. J.; Nagahara, L. A.; Tsui, R. K.; Ramachandran, G. K.; Lindsay, S. M. *Appl. Phys. Lett.* **2002**, *81*, 3043.
- (28) Rawlett, A. M.; Hopson, T. J.; Amlani, I.; Zhang, R.; Tresek, J.; Nagahara, L. A.; Tsui, R. K.; Goronkin, H. *Nanotechnology* **2003**, *14*, 377.
- (29) Kratochvilova, I.; Kocirik, M.; Zambova, A.; Mbindyo, J.; Mallouk, T. E.; Mayer, T. S. *J. Mater. Chem.* **2002**, *12*, 2927.
- (30) Blum, A. S.; Kushmerick, J. G.; Long, D. P.; Patterson, C. H.; Yang, J. C.; Henderson, J. C.; Yao, Y. X.; Tour, J. M.; Shashidhar, R.; Ratna, B. R. *Nat. Mater.* **2005**, *4*, 167.
- (31) Seminario, J. M.; Zacarias, A. G.; Tour, J. M. *J. Am. Chem. Soc.* **2000**, *122*, 3015.
- (32) Di Ventra, M.; Kim, S. G.; Pantelides, S. T.; Lang, N. D. *Phys. Rev. Lett.* **2001**, *86*, 288.
- (33) Cornil, J.; Karzazi, Y.; Brédas, J. L. *J. Am. Chem. Soc.* **2002**, *124*, 3516.
- (34) Lang, N. D.; Avouris, P. *Phys. Rev. B* **2000**, *62*, 7325.
- (35) Seminario, J. M.; Zacarias, A. G.; Tour, J. M. *J. Am. Chem. Soc.* **1998**, *120*, 3970.
- (36) Sellers, H.; Ulman, A.; Shnidman, Y.; Eilers, J. E. *J. Am. Chem. Soc.* **1993**, *115*, 9389.
- (37) Tao, Y.-T.; Wu, C.-C.; Eu, J.-Y.; Lin, W.-L. *Langmuir* **1997**, *13*, 4018.

- (38) Bauschlicher, C. W. J.; Ricca, A.; Mingo, N.; Lawson, J. *Chem. Phys. Lett.* **2003**, *372*, 723.
- (39) Hwang, J.-J.; Tour, J. M. *Tetrahedron* **2002**, *58*, 10387.
- (40) Ciszek, J. W.; Tour, J. M. *Tetrahedron Lett.* **2004**, *45*, 2801.
- (41) Maya, F.; Flatt, A. K.; Stewart, M. P.; Shen, D. E.; Tour, J. M. *Chem. Mater.* **2004**, *16*, 2987.
- (42) Price, D. W.; Dirk, S. M.; Maya, F.; Tour, J. M. *Tetrahedron* **2003**, *59*, 2497.
- (43) Yao, Y.; Tour, J. M. *Org. Chem.* **1999**, *64*, 1968.
- (44) The on/off ratios for each molecule are strongly dependent on the host matrix. See refs 5–8 for molecules 1 and 2, ref 9 for molecule 3, and ref 57 for molecule 4.
- (45) Nuzzo, R. G.; Dubois, L. H.; Allara, D. L. *J. Am. Chem. Soc.* **1990**, *112*, 558.
- (46) Donhauser, Z. J.; Weiss, P. S.; Price, D. W.; Tour, J. M. *J. Am. Chem. Soc.* **2003**, *125*, 11462.

Molecules		ON state	OFF state	Apparent height change (Å)
A	 1	 86 Å x 86 Å		$3.6 \pm 0.7$
B	 2	 86 Å x 86 Å		$3.3 \pm 1.5$
C	 3	 28 Å x 28 Å		$5.1 \pm 1.2$
D	 4	 80 Å x 80 Å		$5.8 \pm 0.7$
E	 5	 86 Å x 86 Å		$1.7 \pm 1.3$
F	 6	 86 Å x 86 Å		$3.4 \pm 1.9$

**Figure 1.** Molecular structures, extracted images of molecules isolated in alkanethiolate SAMs in both “on” and “off” conductance states, and the average measured differences in apparent heights between states (matrix dependent) for each type of inserted molecule. Apparent heights listed for (A) and (B) are from previously published works for these molecules inserted in a dodecanethiolate SAM.<sup>6</sup> (A) Nitro-functionalized OPE molecule<sup>5,6,39</sup> **1** in a decanethiolate SAM from a 153 frame sequence of images, 2000 Å × 2000 Å imaged area with 26 molecules analyzed,  $V_{\text{sample}} = -1$  V,  $I_{\text{tunnel}} = 2$  pA. (B) Unfunctionalized OPE molecule<sup>5,6,39</sup> **2** in a decanethiolate SAM from a 175 frame sequence of images, 2000 Å × 2000 Å imaged area with 26 molecules analyzed,  $V_{\text{sample}} = -1$  V,  $I_{\text{tunnel}} = 2$  pA. (C) Phenanthrene-based molecule<sup>9,40</sup> **3** in an octanethiolate SAM from a 300 frame sequence of images, 1200 Å × 1200 Å imaged area with 13 molecules analyzed,  $V_{\text{sample}} = -1$  V,  $I_{\text{tunnel}} = 3$  pA. (D) Disulfide OPE molecule **4**, prepared by oxidative homocoupling of the thiol from **1**, in an octanethiolate SAM from a 190 frame sequence of images, 2000 Å × 2000 Å imaged area with 14 molecules analyzed,  $V_{\text{sample}} = -1$  V,  $I_{\text{tunnel}} = 2$  pA. (E) Two-contact OPE molecule<sup>41,42</sup> **5** in a dodecanethiolate SAM from a 200 frame sequence of images, 2000 Å × 2000 Å imaged area with 36 molecules analyzed,  $V_{\text{sample}} = -1$  V,  $I_{\text{tunnel}} = 1$  pA. (F) Caltrop<sup>43</sup> molecule in a dodecanethiolate SAM from a 173 frame sequence of images, 2000 Å × 2000 Å imaged area with 15 molecules analyzed,  $V_{\text{sample}} = -1$  V,  $I_{\text{tunnel}} = 1$  pA.<sup>44</sup>

To insert each conjugated molecule (Figure 1) into the host SAMs, a 0.1  $\mu\text{M}$  solution of each molecule was prepared in dry tetrahydrofuran

in a nitrogen environment. For molecules synthesized with a thioacetyl protecting group (indicated in Figure 1 with the abbreviation SAc),

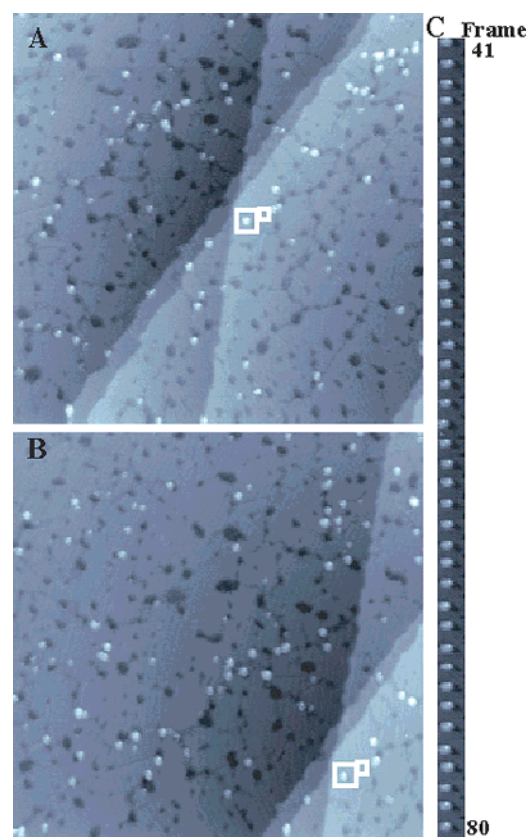


aqueous ammonia was added to hydrolyze the acetate, generating a thiol in situ, allowing the conjugated molecules to adsorb to the Au surface at SAM defect sites.<sup>47,48</sup>

The SAMs were exposed to the insertion solution for times ranging from a few seconds to 0.5 h. In general, more time was allowed for thioacetyl end groups than thiol end groups and more time was allowed for larger, branched molecules to insert. No significant differences were observed with STM between the protected and unprotected thiols; some deprotection is expected via direct surface reaction. Each substrate was dried under a stream of nitrogen after insertion and stored at room temperature in a desiccator until imaging.

Insertion occurs at defect sites such as domain boundaries, step edges, and substrate vacancy defects in the host matrix. Molecules were shown to be isolated in the host SAM using STM images recorded with molecular resolution of the surrounding matrix; the inserted molecules appear in the SAM, each with the same shape indicative of a feature smaller than the tip being imaged.<sup>22</sup> The STM topography images recorded for these molecules are convolutions of the geometries and conductivities of the molecules; therefore, because these molecules are both more conductive and physically thicker than the host SAMs, they appear as protrusions in STM images.<sup>22,49</sup> Larger bundles of these molecules are also imaged and appear broader, indicating insertion of both isolated single molecules and bundles of molecules in single samples.<sup>49</sup> The number of molecules inserted together can be controlled to some extent by controlling the tightness (quality) of the SAM matrix.

**Apparent Height Determination.** All STM imaging presented here was performed in either of two ambient-condition, custom-built microscopes with high mechanical and temperature stability, and high current sensitivity, as described previously.<sup>50</sup> Successive STM images were acquired over the same area for several (up to 30) hours to determine the behavior of the molecules inserted into host matrixes. Relatively large scan areas were acquired so that the activity of tens of isolated molecules could be recorded simultaneously, and, in addition, many high-resolution time-lapse series of images have been recorded. Piezoelectric drift from thermal fluctuations and piezoelectric creep could change the area imaged, so a tracking algorithm was developed to correct for drift during acquisition and for postacquisition analyses.<sup>51</sup> Several inserted molecules were present in the STM images at domain boundaries, step edges, and substrate vacancy defects. Figure 2A and B shows a 2000 Å × 2000 Å scan area with a single molecule (the same molecule in both images) highlighted (large white box) to illustrate our data extraction procedure. To maintain a consistent background, a second box (adjacent, smaller white box) was extracted proximate to the molecule of interest. The apparent height was taken as the difference of the imaged height of the protrusion and the average of the imaged height of the host matrix background frame. Because the host matrix was subtracted as the background, the change in apparent height between the bistable conductance states is dependent on the imaged height of the host matrix as compared to the imaged height of the inserted molecule. Frames 41–80 extracted for this single molecule appear in Figure 2C. Each molecule in Figure 2A underwent this process to extract the histograms of the apparent heights of the molecules. The differences in apparent heights between the “on” and “off” states are listed in Figure 1. For the apparent height histograms, the number of molecules analyzed ranged from 13 to 26 molecules analyzed over



**Figure 2.** Molecular tracking process from a series of images (2000 Å × 2000 Å,  $V_{\text{sample}} = -1$  V,  $I_{\text{tunnel}} = 2$  pA) of an octanethiolate SAM with inserted nitro-functionalized OPE molecules **1**, with background correction. (A) and (B) show two frames from this series of images. For each molecule, extracted (larger white box) and background (smaller white box) regions are automatically selected for each frame. The background corresponds to the SAM apparent height near the extracted molecule. (C) Extracted frames 41–80 from the molecule highlighted in (A) and (B) with corrected background.

153–200 frames. Also displayed in Figure 1 are example extracted images of the “on” and “off” conductance states for each type of molecule. For all molecules studied, switching was reversible, stochastic, and molecules in the “off” state still appeared as slight protrusions, indicating that switching was not occurring through molecular displacement.

For switching analyses, we typically record image areas of (1000–2000 Å)<sup>2</sup> to characterize as many molecules as possible while retaining sufficient resolution. At this scale and at our typical scan line density, the STM tip scanned over a molecule 2–4 times per image (accumulating a total of 5–10 image pixels to represent the molecule, where each pixel represents sampling on a millisecond time scale); thus, the switching activity of a single molecule was not recorded during the majority of each image, but multiple measurements of each molecule were collected in each image.

## Results and Discussion

Figure 1 presents the conjugated molecules we have inserted into host SAMs to test the proposed switching mechanisms using STM. Molecules **1** and **2** have previously been analyzed and discussed.<sup>5–7</sup> They are included here to complete the analyses and testing of the proposed mechanisms. We will discuss how each molecule listed in Figure 1 tests proposed mechanisms for conductance switching when inserted into host *n*-alkanethiolate matrixes. The scanning parameters and host matrixes for each molecule are listed in the caption for Figure 1.

(47) Cai, L. T.; Yao, Y. X.; Yang, J. P.; Price, D. W.; Tour, J. M. *Chem. Mater.* **2002**, *14*, 2905.

(48) Tour, J. M.; Jones, L.; Pearson, D. L.; Lamba, J. J. S.; Burgin, T. P.; Whitesides, G. M.; Allara, D. L.; Parikh, A. N.; Atre, S. V. *J. Am. Chem. Soc.* **1995**, *117*, 9529.

(49) Bumm, L. A.; Arnold, J. J.; Cygan, M. T.; Dunbar, T. D.; Burgin, T. P.; Jones, L.; Allara, D. L.; Tour, J. M.; Weiss, P. S. *Science* **1996**, *271*, 1705.

(50) Bumm, L. A.; Arnold, J. J.; Charles, L. F.; Dunbar, T. D.; Allara, D. L.; Weiss, P. S. *J. Am. Chem. Soc.* **1999**, *121*, 8017.

(51) Mantoosh, B. A.; Donhauser, Z. J.; Kelly, K. F.; Weiss, P. S. *Rev. Sci. Instrum.* **2002**, *73*, 313.

**Functional Group Reduction and Functional Group Rotation Mechanisms.** Seminario and co-workers have suggested that applying a reducing potential to OPE functionalized molecules with both nitro- and amine-groups can in principle reduce the molecule, thereby extending the lowest unoccupied molecular orbital (LUMO) over the molecule and increasing conduction.<sup>31</sup> This scheme requires potentials high enough (calculated at 0 K to be 1.74 V) to reduce the molecule for the conductance change to occur.<sup>31</sup> Similarly, for the functional group rotation scheme, a change in the molecular orbitals was hypothesized by Lang and co-workers to change the conductance. Here, the highest occupied molecular orbital (HOMO) to LUMO gap would be changed, dependent on the rotation of a nitro-functional group, with respect to the phenyl ring to which it is bonded, modulating conduction through the molecule.<sup>32</sup> For the conductance to change according to this scheme, it would be necessary to have substituent groups on the conjugated molecule.

These first two hypotheses of functional group reduction and functional group rotation are not consistent with our observations.<sup>5,6,52</sup> Stochastic conductance switching occurs spontaneously at moderate scanning potentials of  $\pm 1$  V sample bias, which are nonreductive potentials, refuting the possibility of reduction causing the observed change in conductance. At higher biases, Donhauser et al. have shown limited ability to control switching events from the “on” to the “off” state, even out of tunneling range where electrons are not supplied for reduction (however, these higher biases can also cause disorder to the surrounding SAM).<sup>5,6</sup> For **2**, Lewis et al. were able to induce switching at low bias by stabilizing the conductance states via intermolecular interactions with the surrounding matrix.<sup>7</sup> Furthermore, as shown in Figure 1A and B, both the functionalized OPE molecule as well as the unfunctionalized (no substituent groups on the phenyl rings) exhibit the same stochastic conductance switching (i.e., exhibit both “on” and “off” states), eliminating functional groups as being required for conductance switching.

**Backbone Ring Rotation Mechanism.** Brédas and co-workers have suggested that inhibition of rotation for the middle OPE phenyl rings would be required for changes in conductance to occur. When all three rings of the OPE molecules are parallel, the conductance would be maximized due to optimal  $\pi$ -orbital overlap; conversely, when the rings are rotated with respect to one another, the conductance would be lower.<sup>33</sup> This theoretical work relies on substituent groups to inhibit rotation; the nature of the substituent group should not matter as long as it is sufficiently bulky to constrict rotation at room temperature. However, the barrier for ring rotation for one benzene ring in the OPE molecules has been theoretically calculated as 0.037 eV, if allowed to rotate freely, but is predicted to be as high as 1.6 eV if the molecule were in a tightly packed undecane matrix.<sup>31,52</sup>

To test this mechanism, the phenanthrene molecule (2-thioacetyl-phenanthrene)<sup>53</sup> **3** was synthesized to fuse aromatic rings together and thus into the same plane, precluding rotation

about the middle bond (an energy in excess of 6 eV would be required for this to occur, and would not be accessible at room temperature). Several extended series of images of areas ranging from  $(1200\text{--}1500\text{ \AA})^2$  over time periods of 10–12 h revealed that the phenanthrene thiolate molecule exhibits two conductance states similar to that observed for previously inserted molecules.<sup>9</sup> The apparent height differences between the “on” and “off” states were determined to be  $5.1 \pm 1.2\text{ \AA}$  in an octanethiolate matrix ( $V_{\text{sample}} = -1\text{ V}$ ,  $I_{\text{tunnel}} = 1\text{ pA}$ ), analyzing 13 molecules over 300 frames. This observation of two conductance states is inconsistent with the model that internal ring-rotation is the mechanism for the conductance switching observed.

**Neighbor Molecule Interactions Mechanism.** Lang and Avouris have calculated a reduction in the conductance of a pair of “carbon wires” at low bias when the wires are closely packed (i.e., between 3-fold hollow sites on Ni{111}) as compared to a single isolated wire.<sup>34</sup> This was attributed to two possible sources. The first was the overlap of  $\pi$ -orbitals between adjacent carbon wires, which was predicted to decrease the effective bond order of the  $\pi$ -bonds via creation of  $\sigma$ -like bonds linking the wires. The second was that of through-electrode (substrate) binding; the electronic charge transferred to the molecules from the electrodes was predicted to decrease.<sup>34</sup> In related work, Seminario et al. calculated that different conformations of a tolane dimer have different conductivities depending on the ring alignment of neighboring rings,<sup>35</sup> while Emberly and Kirczenow have made theoretical calculations comparing single benzenedithiol molecules bridging break junction gaps as compared to overlapping benzenedithiol molecules in break junctions.<sup>54</sup> The magnitude of the current, theoretically calculated, for a single molecule in the break junction exceeds experimental values measured by Reed, Tour, and co-workers,<sup>19</sup> which Emberly and Kirczenow attempted to explain by suggesting that the current can flow through overlapping benzenedithiol molecules with only one molecule attached at each end of the fractured Au wire.<sup>54</sup>

Two molecules in close proximity have the potential to interact, thereby changing the observed conductance. To test how this would affect the observed conductance in our systems, disulfide forms of the nitro-functionalized OPE molecules (4[4-(2-nitro-4-phenylethynyl-phenylethynyl)-benzenethiol]disulfide) **4** were inserted into host octanethiolate SAM matrixes.<sup>55</sup> Nuzzo et al. have shown that disulfide molecules dissociatively chemisorb as thiolates on the Au{111} surface.<sup>56</sup> We also believe that after surface-based dissociation takes place, one or both halves of the molecule adsorb, because we can subsequently image inserted molecules; however, due to the higher conductance and close proximity of the inserted molecules, we could not typically resolve pairs from single molecules. Figure 3 presents imaged heights of inserted OPE molecules where the host octanethiolate SAM matrix has been normalized to 1 Å. Figure 3A and B presents unfunctionalized OPE molecules **2** chemisorbed as thiolates from thiols, where the leftmost inserted molecule is in the “on” state in Figure 3A and in the “off” state in Figure 3B, while the rightmost molecule remains “on” in both images. Figure 3C and D shows nitro-functional-

(52) Seminario, J. M.; Derosa, P. A.; Bastos, J. L. *J. Am. Chem. Soc.* **2002**, *124*, 10266.

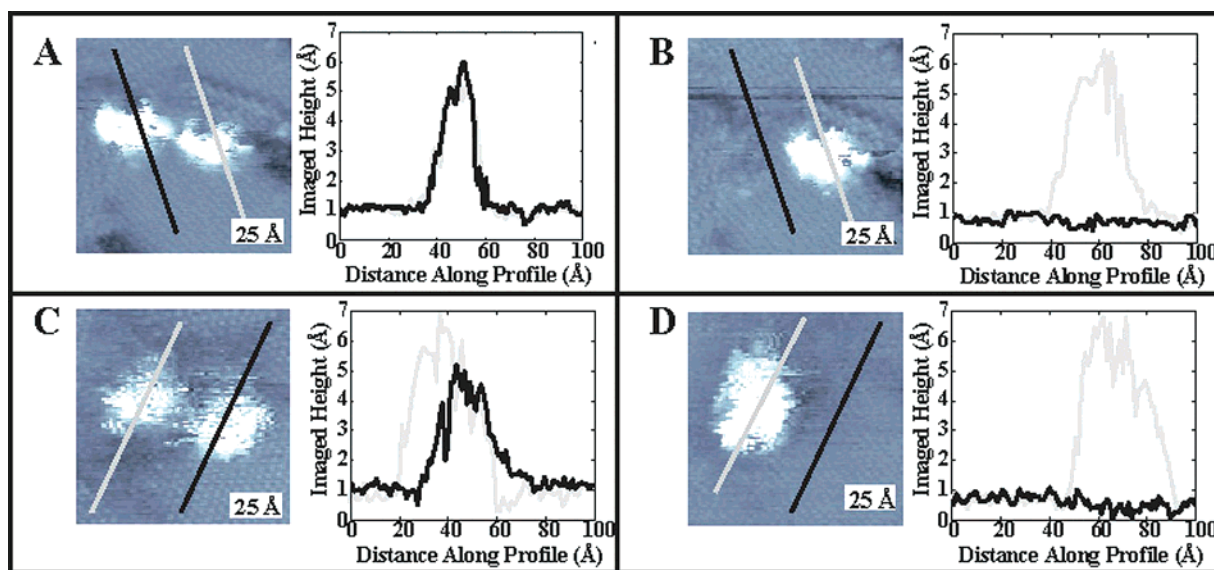
(53) Molecule naming schemes were obtained from Chemdraw (CambridgeSoft, 5.0 ed.; CambridgeSoft Corp.: Cambridge, MA, 1998) and Beilstein Commander (GmbH, M. I. S., 4.0 ed.; MDL Information Systems GmbH: Frankfurt, Germany, 2000.)

(54) Emberly, E. G.; Kirczenow, G. *Phys. Rev. B* **2001**, *64*, 235412.

(55) Insertion into a thicker matrix was attempted, but unsuccessful; we attribute this to steric hindrance where the disulfide bond is unable to access the substrate and thus unable to chemisorb dissociatively.

(56) Nuzzo, R. G.; Zegarski, B. R.; Dubois, L. H. *J. Am. Chem. Soc.* **1987**, *109*, 733.





**Figure 3.** Comparison of apparent heights for molecules inserted as monothiolates (A) and (B) versus those inserted as disulfides (presumably as pairs) (C) and (D). Here, we show extracted inserted frames for inserted molecules and corresponding line scans (lines through images correspond to associated line scans shown) for (A) and (B) unfunctionalized OPE molecule **2** thiolates inserted as thiolates ( $V_{\text{sample}} = -1$  V,  $I_{\text{tunnel}} = 2$  pA,  $100 \text{ Å} \times 100 \text{ Å}$  extracted area) and (C) and (D) dimerized OPE molecule thiolates inserted from disulfides **4** (presumably as pairs) ( $V_{\text{sample}} = -1$  V,  $I_{\text{tunnel}} = 2$  pA,  $100 \text{ Å} \times 100 \text{ Å}$  extracted area). (A) Both unfunctionalized OPE molecules appear in the “on” state with apparent heights of  $\sim 4.5$  Å. (B) The leftmost unfunctionalized OPE molecule has switched into the “off” conductance state with an apparent height of  $\sim 0$  Å. (C) Both dimerized pairs of OPE molecules appear in the “on” state with apparent heights averaging  $\sim 4.5$  Å. (D) The rightmost dimerized pair of OPE molecules has switched into the “off” conductance state with an apparent height of  $\sim 0$  Å. Note that the individual molecules of the dimers were not resolved here.

ized OPE molecules chemisorbed as thiolates from disulfides **4**, presumably inserted as pairs. The rightmost molecules exhibit conductance switching from the “on” state to the “off” state from Figure 3C to D, while the leftmost molecules remain in the “on” conductance state. The apparent heights (the imaged height minus the background height, here  $\sim 4.5$  Å) for both the dimer thiolate molecules and the single thiolate molecules that switch have no significant variation. The average apparent heights for molecules adsorbed as pairs fall within the statistical distributions of our previous measurements analyzing single molecules.<sup>57</sup> No significant differences in conductances were observed for the molecules inserted as pairs, spontaneously formed pairs, or those existing as individuals, thus eliminating neighbor molecule interactions as a mechanism for conductance switching. The observation of not having neighboring molecule interactions is consistent with other experimental data.<sup>58–60</sup>

**Bond Fluctuation Mechanism.** STM measurements performed by Lindsay and co-workers analyzed conductance switching for inserted  $\alpha,\omega$ -dithiol OPE molecules with nanoparticles attached to the pendant thiol at the film interface. They hypothesized that these OPE molecules detaching from the surface caused the observed conductance changes where the nanoparticle is not present in the image.<sup>11</sup> This hypothesis assumed that the nanoparticle must be covalently attached to the surface to be imaged or in the “on” conductance state and,

conversely, detached from the substrate to be in the “off” conductance state.

Figure 4 shows images of 1.5 nm dodecanethiolate-passivated Au nanoparticles deposited onto a dodecanethiolate SAM formed on a Au{111} substrate.<sup>61</sup> No covalent attachment was possible between these nanoparticles and the underlying Au{111} surface; however, Figure 4A shows that STM imaging of these particles was nonetheless possible. Nanoparticles that are not covalently attached to the underlying substrate are easily displaced by the STM tip and appear as streaks in STM images. Figure 4A and B shows successive images where the area for Figure 4B is indicated by the white box in Figure 4A. These sequential images show that a region that initially had a high coverage of noncovalently attached nanoparticles had a relatively low coverage after the STM tip imaged the area, thereby sweeping away the nanoparticles. Figure 4C shows that a noncovalently attached nanoparticle (indicated by the arrow) may be immobilized (stable) on a SAM surface (presumably through interdigitation of the decanethiolate ligand shell with the SAM). The presence of a covalent bond with the underlying surface is not necessary to image the nanoparticle with STM. This is contrary to the assumption made in the assignment of the bond fluctuation mechanism by Lindsay and co-workers.<sup>11</sup> Instead, it appears that under the harsher tunneling conditions used in their work (i.e., smaller tip–sample separations), Lindsay and co-workers mechanically disrupted the tethered nanoparticles.<sup>62</sup>

**Hybridization Change Mechanism.** We have previously suggested that a change in hybridization between the conjugated molecules and the substrate results in the observed changes in

(57) As a general observation, molecules inserted from the dimerized version of the nitro-functionalized OPE exhibit switching events more frequently than do single molecules. This is likely a consequence of the bias in our experiment; we require relatively larger defects in the matrix to enable access and dissociate chemisorption of the disulfide molecules (vs thiol) to the substrate. We have previously shown that the rigidity of the matrix around the switches determines the frequency of switching.

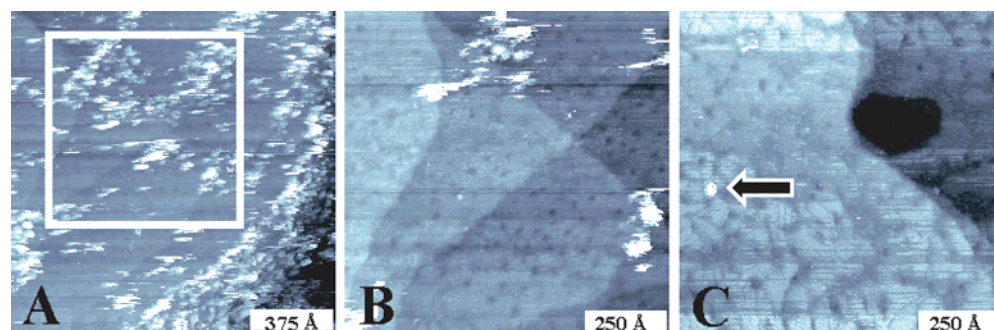
(58) Kushmerick, J. G.; Naciri, J.; Yang, J. C.; Shashidhar, R. *Nano Lett.* **2003**, *3*, 897.

(59) Xu, B.; Tao, N. J. *Science* **2003**, *301*, 1221.

(60) Cui, X. D.; Primak, A.; Zarate, X.; Tomfohr, J.; Sankey, O. F.; Moore, A. L.; Moore, T. A.; Gust, D.; Harris, G.; Lindsay, S. M. *Science* **2001**, *294*, 571.

(61) Hostetler, M. J.; Wingate, J. E.; Zhong, C.-J.; Harris, J. E.; Vachet, R. W.; D., C. M.; Londono, J. D.; Green, S. J.; Stokes, J. J.; Wignall, G. D.; Glush, G. L.; Porter, M. D.; Evans, N. D.; Murray, R. W. *Langmuir* **1998**, *14*, 17.

(62) Mantooh, B. A.; Fuchs, D. J.; Smith, R. K.; Dameron, A. A.; Moore, A. M.; Weiss, P. S., in preparation.



**Figure 4.** STM images of 1.5-nm dodecanethiolate-stabilized nanoparticles<sup>61</sup> deposited onto a dodecanethiolate SAM; imaging conditions:  $V_{\text{sample}} = -1$  V,  $I_{\text{tunnel}} = 10$  pA. Images (A) and (B) are sequential images, and the area of (B) is indicated by the white box in (A). (A) Noncovalently attached nanoparticles imaged on a dodecanethiolate SAM,  $1500 \text{ \AA} \times 1500 \text{ \AA}$ . The streaks in the horizontal direction indicate nanoparticle displacement by the STM tip. (B) Particles swept away by the STM tip no longer appear in the image,  $1000 \text{ \AA} \times 1000 \text{ \AA}$ . (C) A single nanoparticle (arrow), with an apparent height of  $14.9 \text{ \AA}$ , sufficiently immobilized on the SAM to be imaged,  $1000 \text{ \AA} \times 1000 \text{ \AA}$ .

conductance.<sup>1,5–8</sup> Similar ideas were put forth by Kornilovitch and Bratkovsky.<sup>63</sup> The contacts of organic molecules to electrodes can have a large influence on the conductance observed through the molecule. For self-assembly techniques, covalent attachment of organic molecules to metal substrates, commonly achieved through thiolate end-groups to Au{111} substrates, form well-ordered SAMs.<sup>48,64</sup> Other attachment schemes have been realized, including various combinations of transition metal and semiconductor substrates with other molecular end-groups such as selenolates<sup>65</sup> and isonitriles.<sup>13</sup>

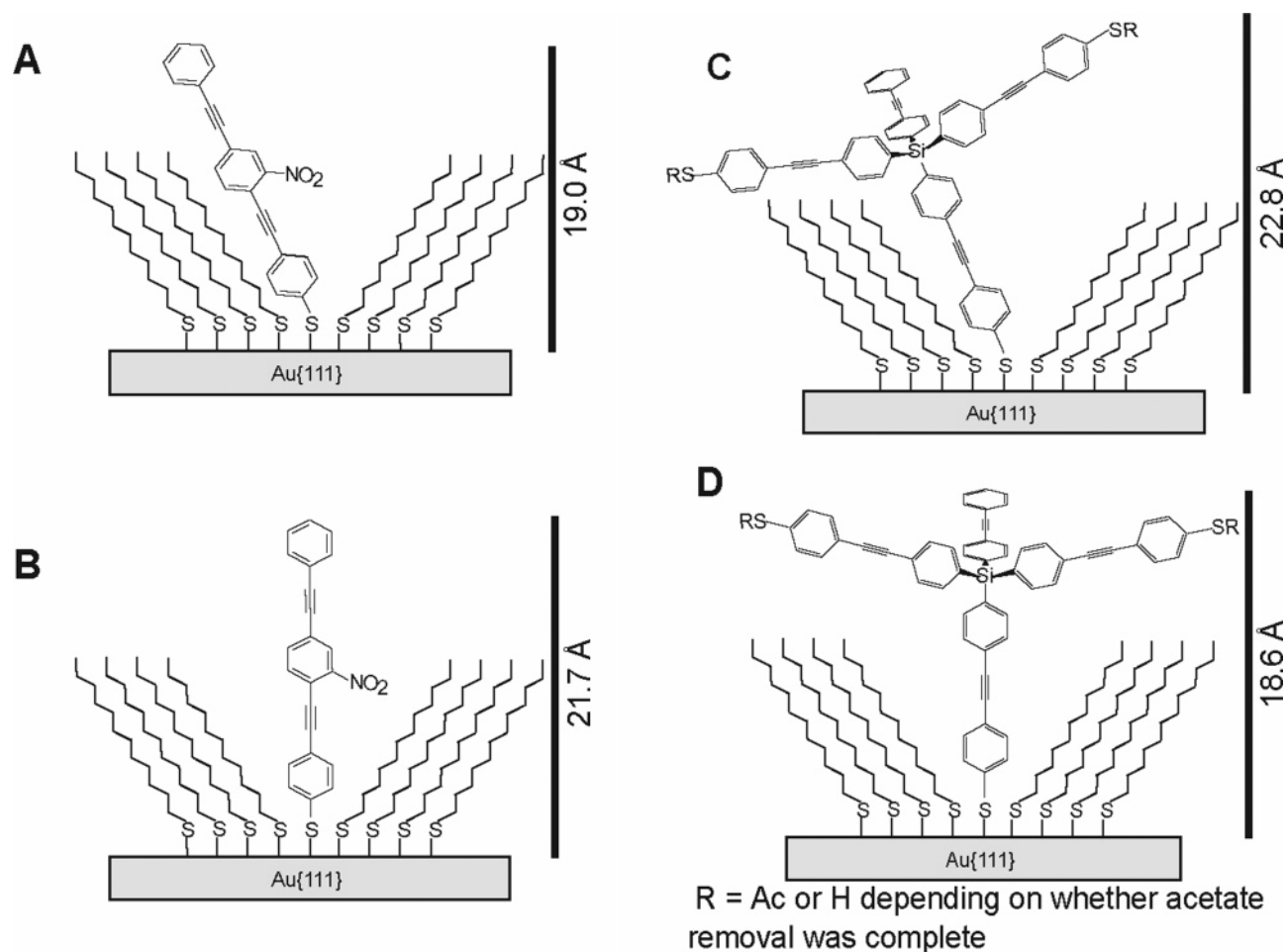
We have experimentally observed conductance switching using STM for each of the molecules in Figure 1. Each of these molecules has been engineered to test various hypotheses for conductance switching. What has not changed in our molecular design is the S–Au bonding scheme. In the hybridization change mechanism, the metal–molecule system must have enough degrees of freedom to change the structure of the metal–molecule bond. The packing of the matrix around the inserted molecule inhibits the motion of the molecules. We previously showed that tightening or using more rigid matrixes leads to longer persistence times in a particular conductance state.<sup>5–7</sup> Also, if a particular hybridization is favored, a larger ratio of that conformation should be observed. This is difficult to measure quantitatively with STM because some molecules in the “off” conductance state are not easily imaged and thus the measurements are biased toward the “on” state. The change in hybridization (i.e., change in the tilt or substrate reconstruction) is concurrent with changing  $\pi$ -interactions between the molecule and the gold substrate, as predicted theoretically.<sup>63,66</sup> A higher degree of overlap was predicted when the molecule is tilted rather than perpendicular with the surface, and therefore higher conductance has been predicted for tilted molecules.<sup>36,37</sup> However, from driven motion, we infer that the configuration in which the molecule is oriented more normal to the surface corresponds to the “on” state, and the more tilted configuration corresponds to the “off” state.<sup>7,8</sup> This assignment was confirmed by redesigning switch molecules to have the opposite dipole orientation and showing that the induced switching via applied electric field changed to having the opposite polarity.<sup>8</sup>

**Restricted Molecular Motion.** Molecules with two or three possible surface contacts, (thioacetic acid S-{4-[3’-(4-acetyl-sulfanyl-phenylethynyl)-4’,6’-bis-phenylethynyl-[1,1’,3’,1’]terphenyl-3-ylethynyl]-phenyl}ester) “two-contact”<sup>42</sup> **5** or the caltrop<sup>43</sup> **6**, respectively, would have less ability to move and thus reduced switching activity if each contact were bound. Also, if multiple thiols attach to the gold, this would inhibit switching unless hybridization changes occur at each attachment. Due to the rigidity of the molecular designs, tilt would be limited to one plane if two thiols attached, reducing the observed switching events. Multiple attachments could also give insight into how the conductance is affected by having multiple conduction pathways, similar to neighboring molecule interactions.

In our experiments, we infer that it is most likely that only one attachment was able to form, because the spacing between the thiols does not adequately match the binding site spacing between gold substrate atoms. We would expect the registry to be close to that of the host alkanethiolate monolayer preassembled on the Au{111} substrate. For similar “two-contact” molecules, Maya et al. found that “two-contact” molecules had two energy minima: one in a “U-shaped” conformation, and the second in a zigzag conformation due to free rotation of the terphenyl backbone.<sup>41</sup> Due to steric hindrance caused by the preassembled host SAM, it is most likely that the molecules we observe have inserted in the zigzag conformation, although it is possible for two contacts to bind to the surface.<sup>41</sup> Furthermore, it is unlikely (but in principle possible) to have a defect in the host SAM large enough to accommodate molecule **6** with several contacts to the substrate. Design and syntheses of new molecules with two or more contacts matching the gold lattice spacing are in progress.

The switching frequency of the singly contacted, but complex molecule with two possible contacts was similar to that observed for the nitro-functionalized OPE **1** when in a dodecanethiolate host SAM. We reported 32% of nitro-functionalized OPE molecules **1** switching with a measured on/off ratio of 4:1 for a surface coverage of  $12.4 \times 10^{-6}$  molecules/ $\text{\AA}^2$  when in a dodecanethiolate host matrix that had been deposited for 24 h.<sup>5</sup> For the two-contact OPE molecules **5**, we observed 20% of molecules switching with an on/off ratio of 21:5 for a surface coverage of  $11 \times 10^{-6}$  molecules/ $\text{\AA}^2$  in a similar host matrix. The similarity of these results for completely different molecules inserted into similar host matrixes leads us to believe the switching is dependent on something common to both mol-

(63) Kornilovitch, P. E.; Bratkovsky, A. M. *Phys. Rev. B* **2001**, *64*, 195413.  
 (64) Nuzzo, R. G.; Fusco, F. A.; Allara, D. L. *J. Am. Chem. Soc.* **1987**, *109*, 2358.  
 (65) Monnell, J. D.; Stapleton, J. J.; Jackiw, J. J.; Dunbar, T. D.; Reinerth, W. A.; Dirk, S. M.; Tour, J. M.; Weiss, P. S. *J. Phys. Chem. B* **2004**, *108*, 9834.  
 (66) Emberly, E. G.; Kirczenow, G. *Phys. Rev. Lett.* **2003**, *91*, 188301.



**Figure 5.** Schematic of nitro-functionalized OPE **1** and caltrop **6** molecules inserted into dodecanethiolate SAMs. (A, B) Nitro-functionalized OPE molecule in tilted and normal configurations, respectively. (C, D) Caltrop molecule in tilted and normal configurations, respectively. Note that the nitro-functionalized OPE molecule protrudes further from the SAM in the normal conformation, yet, for the caltrop, protrusion from the SAM is largest for the tilted conformation. The nonsurface-bound sulfur groups (shown as SR) could exist as free thiols or as protected thioacetyl groups depending on whether acetate removal was complete.

ecules, that is, their attachment to the surface. The size of the more complex molecule does not appear to affect the measured on/off ratios because the molecules only insert in areas (SAM defect sites) where they have enough degrees of freedom to find favorable conformations.

Under similar conditions, the caltrop molecule **6** displayed switching behavior similar to the nitro-functionalized **1** and two-contact molecules **5** ( $3.7 \times 10^{-6}$  molecules/ $\text{\AA}^2$ ; 4:1 on/off ratio; and 53% exhibiting switching). An interesting observation with the caltrop molecules deals with the issue of the appearance in STM images being a convolution of electronic states and geometric shape. For the nitro-functionalized molecules **1**, a molecule oriented normal to the surface will naturally have a topographic height greater than that of its tilted form (Figure 5A and B). Conversely, if only one leg of the caltrop molecule is attached to the gold substrate, a molecule oriented normal to the surface is physically shorter than when the molecule is tilted due to the tetrahedral geometry (Figure 5C and D). If the observed conductance change were due to physical height alone, the molecules would always protrude from the SAM, and the average apparent height changes (Figure 1) for different molecules in similar matrixes would not be in the same range. We would have expected to observe a trend opposite from that observed for the other molecules inserted; that is, we would

see a higher ratio of molecules in the “off” state. Because this trend was not observed, we look for similarities between the molecules inserted; this again points toward the interaction of the thiol and substrate enabling the observed switching events.

## Conclusions and Prospects

We have designed and studied several different molecules exhibiting stochastic conductance switching. Previous work has demonstrated how the surrounding matrix can influence the frequency of stochastic switching events.<sup>5–8</sup> We have studied a number of proposed mechanisms through engineering the molecular structure to test possible conductance switching mechanisms. The only mechanism consistent with all of our data is that switching is caused by a change in hybridization of the molecule that occurs with a change in the molecule–substrate contact. We have given examples of switching events in molecules that do not allow internal ring rotation, eliminating this as the general mechanism for the conductance changes in these systems. We have also shown conductance switching in several molecules not containing substituent groups, showing that the stochastic conductance switching is not attributable to the roles of the functional groups. All examples given have used highly conjugated molecules adsorbed through S–Au interactions. Further work in our group is currently being performed



521	to analyze different contact interactions, including S–Pd and	Defense Advanced Research Projects Agency, National Institutes	529
522	CN–Au. At this time, all conjugated thiol molecules we have	for Standards and Technology, National Science Foundation,	530
523	inserted into <i>n</i> -alkanethiol matrixes exhibit stochastic conduc-	Air Force Office of Scientific Research, and the Office of Naval	531
524	tance switching.	Research. B.A.M. thanks the American Chemical Society	532
525	<b>Acknowledgment.</b> We would like to thank our long-time	Division of Analytical Chemistry for a fellowship sponsored	533
526	collaborators David Allara and his students for helpful discus-	by GlaxoSmithKline.	534
527	sions and characterization underlying this research. We grate-		
528	fully acknowledge support from the Army Research Office,	JA055761M	535